Sorption and Transport of CO_2 in PVF_2/PMMA Blends

J. S. CHIOU and D. R. PAUL, *Department of Chemical Engineering and Center for Polymer Research, University of Texas, Austin, Texas 78712*

Synopsis

The sorption and transport of CO_2 in miscible PVF_2/PMMA blends are reported at 35°C as a function of pressure from 1 to 25 atm. Significant plasticization by CO_2 is evident for all blend compositions. This effect induced further crystallization of PVF_2 for some blends, altered the shape of sorption isotherms for blends with a glassy amorphous phase, and resulted in permeabilities which increased with pressure for all compositions. Modified sorption and transport models to account for plasticization are used to analyze the data. The effect of crystallinity on observed behavior has been accounted for using approximate models to allow comparison of responses of sorption and transport with blend composition.

INTRODUCTION

Extensive investigations spanning more than a decade have demonstrated that poly(vinylidene fluoride) (PVF_2) and poly(methyl methacrylate) (PMMA) form miscible blends.[1-10] Related studies on the morphology,[11,12] mechanical properties,[12,13] and chemical resistance[13] of this blend system have appeared. To add to this growing body of knowledge, we initiated an investigation of the sorption and transport of gases in these materials. Rather complex relations between these observations and blend composition could be expected since near ambient temperature PMMA is amorphous and glassy while PVF_2 is semicrystalline and rubbery. Thus, variation in blend composition causes changes in the level of crystallinity and the state of the amorphous phase, all of which influence sorption and transport behavior. For reasons outlined below, other levels of complexity appear for this system when the gas is carbon dioxide. Consequently, we have chosen to focus here on CO_2 only and to report the results for other gases separately.

We have recently demonstrated by direct calorimetric measurements[14] that sorption of CO_2 can significantly depress the glass transition temperature of some polymers. This plasticization by dissolved CO_2 can, in certain cases, induce crystallization of the polymer[15] (just as the sorption of liquids or vapors are known[16-22] to do) and alter the nature of the sorption isotherm.[23] Only a few other studies[24,25] have called attention to the potential plasticizing action of gases at high pressure. These issues become important for the PVF_2/PMMA system since some mixtures have glass transition temperatures only slightly above the observation temperature of 35°C, and, thus, depression of T_g by sorption of CO_2 at high pressures can convert their glassy amorphous state into a rubbery one. This has not been an issue in previous studies of sorption and transport in miscible blend systems described in the literature.[26-39]

Journal of Applied Polymer Science, Vol. 32, 2897-2918 (1986)
 CCC 0021-8995/86/012897-22$04.00

In contrast to the behavior for less condensible gases, the results here show that the permeability coefficient for CO_2 increases with pressure for PMMA and all blends with PVF_2. This is not surprising for PVF_2 or blends which have T_g values less than 35°C. However, this response is somewhat unusual for glassy polymers and requires modification of the transport model normally used for such systems. Studies on other glassy polymers which show this effect with CO_2 are in progress and will be reported later.

EXPERIMENTAL

PVF_2 from Pennwalt, Kynar 460N, and PMMA from Rohm and Haas, Plexiglas V(811), were received in pellet form. Films of various blend compositions were prepared by extrusion as described earlier.[13,14] The apparatus and experimental procedures for gas sorption and permeation measurements were the same as used previously.[40,41]

All films were conditioned by exposure to CO_2 at 25 atm for 1 day before making any sorption or permeation measurements. This treatment resulted in no significant dimensional changes in the extruded films which were rich in either PVF_2 or PMMA. However, for some intermediate compositions, especially 35 and 40% by weight of PVF_2, significant rippling of the surface and shrinkage in the machine direction occurred. This caused no problems for sorption measurements but presented serious uniformity problems for permeation experiments. To circumvent this difficulty, film specimens were wrapped around a 1-in. metal rod to restrain shrinkage during CO_2 conditioning. Satisfactory permeation specimens were obtained by this technique.

A Perkin-Elmer Differential Scanning Calorimeter was used to measure the crystallinity and glass transition temperatures for each blend composition. Film orientation was determined using a Gaertner Birefringence Measurement System. Further details are given elsewhere.[14,15]

RESULTS AND DISCUSSION

Characterization

Glass transition temperatures measured by DSC for samples after various treatments are shown in Figure 1 as a function of overall blend composition. The dashed line denotes the temperature, 35°C, at which all sorption and permeation observations were made. Curve A shows the T_g observed for the as-extruded materials. No value could be recorded for pure PVF_2[9,42,43] by DSC. However, it is clear that both pure PVF_2 and its blend containing 20% PMMA have T_g's below 35°C and are in the rubbery state at this temperature. All other compositions are glassy at 35°C. Curve A in Figure 2 shows the crystallinity of the as-extruded film using 22.3 cal/g as the heat of fusion for the 100% crystalline PVF_2.[14,44] Blends containing less than 50% PVF_2 are completely amorphous. As seen in Figure 3, extruded films rich in PMMA have relatively low levels of orientation. On the other hand, PVF_2-rich films are semicrystalline and have high levels of birefringence.

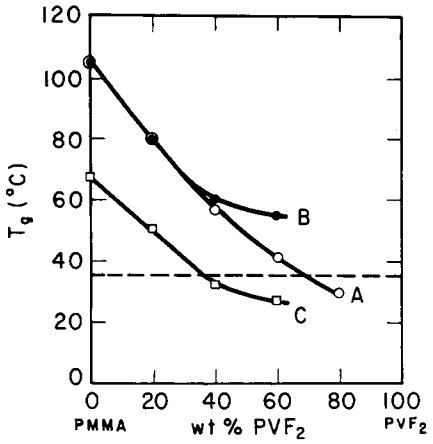

Fig. 1 Glass transition temperature by DSC for PVF_2/PMMA blends: (A) as-extruded; (B) after CO_2 sorption measurements; (C) samples contain CO_2 dissolved to equilibrium at 35°C and 20 atm; (- - -) observation temperature of 35°C.

The significant plasticizing effect of CO_2 is seen by curve C in Figure 1 obtained by DSC measurement on samples still containing CO_2 dissolved to equilibrium at 35°C and 20 atm as reported previously.[14] The T_g's after removal of the CO_2 are given by curve B in Figure 1. The CO_2 plasticization induced further crystallization of PVF_2 as seen by the crystallinity values observed after CO_2 removal, curve B in Figure 2.[15] The birefringence after CO_2 exposure is shown in Figure 3. The reason for the increase in birefringence on exposure to CO_2 is related to growth of oriented PVF_2 crystals as described earlier.[15] The change in the composition of the amorphous phase resulting from additional PVF_2 crystallization on exposure to CO_2 is responsible for the elevation of T_g (curve B relative to curve A) seen in

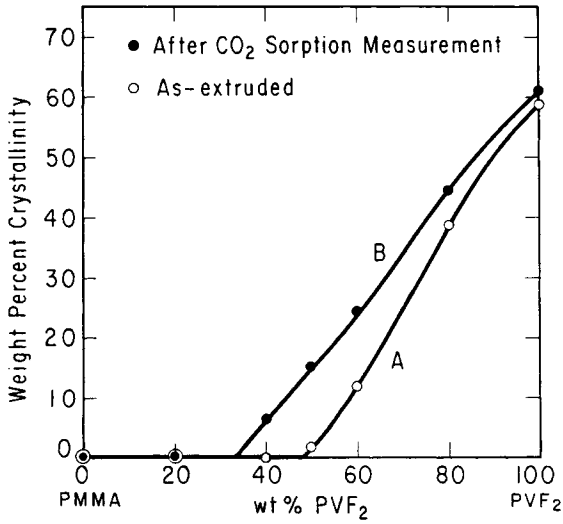

Fig. 2. Crystallinity by DSC for PVF_2/PMMA blends: (●) after CO_2 sorption measurement; (○) as extruded.

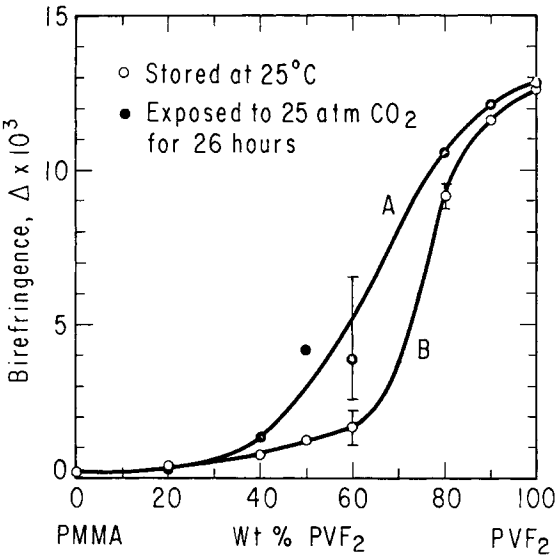

Fig. 3. Birefringence of extruded PVF_2/PMMA film before and after CO_2 exposure: (○) stored at 25°C; (●) exposed to 25 atm CO_2 for 26 h.

Figure 1. The curves B in Figures 1 and 2 are the appropriate ones to use in connection with interpretations of samples used for CO_2 sorption and transport experiments since the initial CO_2 exposure altered the crystallinity level. Figures 1–3 explain why CO_2 conditioning causes dimensional changes to occur in films having intermediate PVF_2 contents. Films rich in PMMA remain glassy when exposed to CO_2 while PVF_2-rich films were already rubbery but highly crystalline.

Sorption

Experimental sorption isotherms for CO_2 at 35°C in PVF_2/PMMA blends are shown in Figure 4. For PVF_2 and the blend containing 80% PVF_2, the isotherms are linear and may be described by Henry's law

$$C = k_D p \tag{1}$$

where C is the concentration of CO_2 in the polymer at equilibrium with a CO_2 pressure p in the gas phase and k_D is the solubility coefficient. This response is the expected one since the amorphous phase of these materials is in the rubbery state at 35°C as seen in Figure 1. On the other hand, the isotherms for PMMA and the 20% PVF_2 blend are concave to the pressure axis which is typical for glassy polymers like these materials. Such isotherms are well described by the following dual mode sorption equation[45,46]

$$C = k_D p + C'_H bp/(1 + bp) \tag{2}$$

where the C'_H parameter corresponds to a Langmuir site capacity and b is a hole affinity parameter according to a simple physical interpretation of the extra term in eq. (2). The first term corresponds to a Henry's law mode like that given by eq. (1).

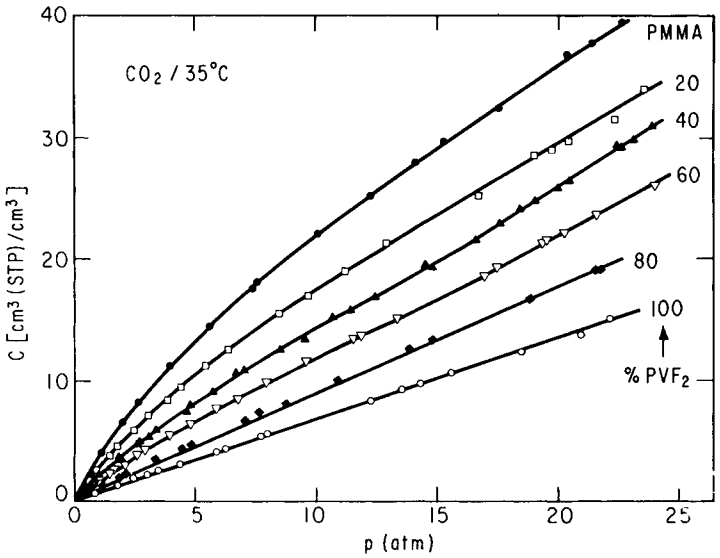

Fig. 4. Sorption isotherms for CO_2 in PVF_2/PMMA blends at 35°C.

Blends of intermediate composition exhibit a more unusual isotherm shape which has been reported earlier[23] for polymers whose T_g is only slightly above the observation temperature. At low pressures, the isotherms for the 40 and 60% PVF_2 blends are concave as expected for glassy polymers. However, this curvature ceases at about 14 atm (60% PVF_2) and 16 atm (40% PVF_2). At higher pressures the isotherms become effectively linear and extrapolate to the origin. This is seen more clearly for the 35 and 50% PVF_2 blends whose isotherms have been plotted separately on a different scale in Figure 5. As described earlier,[23] there is convincing evidence that

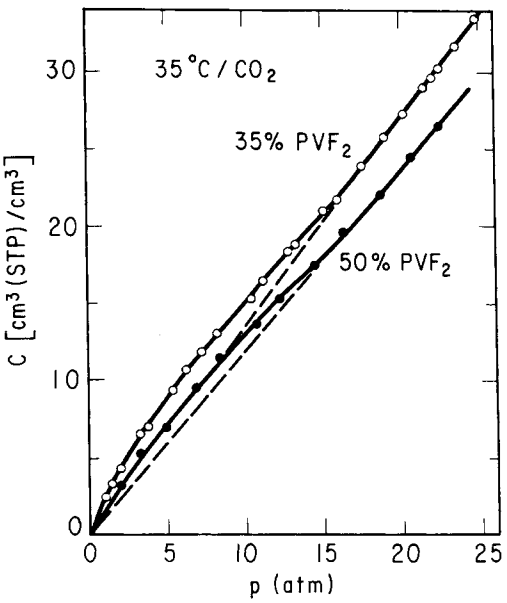

Fig. 5. Sorption isotherms for CO_2 in 35% and 50% PVF_2 blends at 35°C.

for these initially glassy polymers CO_2 plasticization causes a reduction in T_g to the observation temperature at a pressure which is within the range employed in the sorption experiment. Thus, below this pressure the isotherms are curved as expected for glassy polymers, whereas above this pressure the isotherms are linear as expected for rubbery polymers. In terms of eq. (2), CO_2 plasticization eliminates the Langmuir term. The low pressure data for the 80% PVF_2 blend lie slightly above the straight line drawn presumably because the T_g for this material is slightly above 35°C following CO_2 conditioning.

Modified Dual Mode Sorption Model

Because of the variation in crystallinity or amorphous fraction of these blends seen in Figure 2 and the significant plasticizing effect of CO_2 described above, eqs. (1) and (2) cannot be used directly to extract parameters for sorption behavior of the various blends which can be meaningfully compared. However, as seen here, some relatively simple modifications can be made which to a first approximation remove these difficulties.

Earlier papers[33,34,47-51] suggest that the Langmuir type contribution to the sorption isotherm shape given by eq. (2) stems from the nonequilibrium nature of the glassy state. In fact, correlations of data for numerous polymers show that to an excellent approximation the capacity C'_H is proportional to the difference in the poymer T_g and the observation temperature T, i.e., $(T_g - T)$. This suggests that we replace the constant C'_H in eq. (2) by the following:

$$C'_H = C'_{H0}\left(\frac{T_g - T}{T_{g0} - T}\right) \tag{3}$$

where T_g is the glass transition for the polymer containing an equilibrium amount of CO_2 at pressure p, T_{g0} is the transition temperature in the absence of CO_2, and C'_{H0} is the initial Langmuir capacity prior to any reduction in T_g by CO_2 plasticization. Thus, eq. (3) imparts a pressure dependence to the capacity term, and it becomes zero when $T_g = T$ as observed experimentally by varying T[46,50] or by varying T_g.[39,50,52] When T_g is considerably larger than T, this modification is not needed because any reduction in T_g by CO_2 plasticization will cause only a minor change in $(T_g - T)$ relative to $(T_{g0} - T)$; however, it assumes greater importance when T_g is only slightly larger than T as in the case considered here. We assume that plasticization by CO_2 has a negligible effect on k_D and b which seems justified on the basis of available information.[50]

Although we have been able to measure by direct experimental methods[14] the T_g for polymers containing dissolved CO_2, it would be most convenient for present purposes to have a method for calculating the change in T_g as a function of CO_2 content in the polymer. Chow[53] has developed a theoretical relation

$$\ln(T_g/T_{g0}) = \beta[(1 - \theta)\ln(1 - \theta) + \theta \ln \theta] \tag{4}$$

where β is a physical constant and θ is a measure of diluent concentration as defined by

$$\theta = \frac{M_p}{zM_d} \frac{w}{1 - w} \tag{5}$$

and

$$\beta = \frac{zR}{M_p \Delta C_p} \tag{6}$$

where z is the lattice coordinate number, R is the gas constant, ΔC_p is the increase of the specific heat at the glass transition, w is the mass fraction of the diluent, while M_p and M_d are the molecular weights of the repeat unit of the polymer and the diluent, respectively. The appropriate parameters for PVF_2/PMMA blends used here are listed in Table I. For the gas–polymer system studied here, the T_g's calculated from the Chow equation are quite close to the measured ones if $z = 1$.[14]

For semicrystalline polymers, diluents like CO_2 only dissolve in the amorphous phase.[54,55] Thus, eqs. (1) and (2) can be made more useful by expressing the concentration of gas on a unit volume of amorphous polymer. This may be done by dividing either equation by the volume fraction of the amorphous phase α, which for the present systems can be computed from the data in Figure 2. Equation (2) can be written in the final modified form

$$\frac{C}{\alpha} = \left(\frac{k_D}{\alpha}\right) p + \left(\frac{C'_{H0}}{\alpha}\right) \left(\frac{T_g - T}{T_{g0} - T}\right) \left(\frac{bp}{1 + bp}\right) \tag{7}$$

where C/α is the concentration of gas per unit volume of amorphous polymer and (k_D/α) and (C'_{H0}/α) are sorption parameters on a comparable basis. It is these parameters which should be used in any comparisons among different polymers. No modification of b is needed.

TABLE I
Physical Parameters of Glassy PVF_2/PMMA Blends Used for Calculation of Sorption Parameters

% PVF_2	ΔC_P (cal/g °C)	T_{g0}[a]	M_p[b] (g/mol)
60	0.0447	55	79.0
50	0.0503	57[c]	81.2
40	0.0570	60	83.1
35	0.0590[c]	64[c]	84.6
20	0.0664	80	89.9
0	0.0746	105	100.0

[a] Measured by DSC after CO_2 sorption.
[b] Molar average molecular weight.
[c] Interpolated value.

A computer regression analysis program was developed for obtaining (k_D/α), (C'_{H0}/α), and b from the best fit of eq. (7) to the experimental isotherm data. Values for α were computed from curve B in Figure 2. For each pressure, the term $(T_g - T)/(T_{g0} - T)$ was computed from eqs. (4)–(6) using the experimentally determined concentration of CO_2 in the amorphous phase and a typical example is given in Table II. For isotherms having shapes like that shown in Figure 5, a value for (k_D/α) can also be computed directly from the slope of the linear portion of the isotherm. The sorption parameters deduced from the data shown in Figures 4 and 5 are listed in Table III. Where comparisons are possible, the (k_D/α) values obtained by the two methods agree within 4% in two cases and 9% in another.

Figure 6 shows a simple way to understand the effect plasticization has on the sorption isotherm in terms of the models used here. The amount of sorption accounted for by the Langmuir mode, C_H, has been plotted vs. pressure using the modified capacity term from eq. (3) and assuming no change from the initial value, C'_{H0}, all for the case of the 35% PVF_2 blend. In the ideal case, (C_H/α) increases continuously and asymptotically approaches $(C'_{H0})/\alpha)$ at high pressures. Incorporation of the modification for plasticization substantially reduces the sorption by this mode and eventually causes it to decrease and subsequently go to zero. The pressure at which this occurs corresponds to T_g becoming equal to T. Computed and measured values for this pressure agree quite well.

Previous analyses[33,34,39] have interpreted the variation of the Henry's law parameter with blend composition in terms of a model based on a ternary mixture model derived from the Flory–Huggins theory. Adapting this the-

TABLE II
Experimental and Calculated Soption Information for CO_2 in 35% PVF_2 Blend at 35°C

p (atm)	C/α[a] [cm³ (STP)/ cm³ amor polym]	T_g[b] (°C)	$\frac{T_g - T}{T_{g0} - T}$	C'_H/α[c] [cm³ (STP)/ cm³ amor polym]	C_H/α[d] [cm³ (STP)/ cm³ amor polym]
0	0	64	1.0	10.9	0
1.04	2.52	58.5	0.809	8.80	1.02
1.55	3.47	46.8	0.752	8.18	1.34
2.03	4.38	55.3	0.701	7.63	1.56
3.39	6.75	51.8	0.579	6.30	1.89
3.82	7.24	51.1	0.555	6.04	1.97
5.43	9.69	47.9	0.444	4.82	1.97
6.27	10.92	46.3	0.391	4.25	1.88
7.28	12.21	44.8	0.338	3.68	1.76
8.38	13.49	43.3	0.288	3.13	1.61
10.50	15.82	40.8	0.200	2.18	1.24
11.27	16.96	39.6	0.159	1.73	1.02
12.92	18.92	37.6	0.091	0.99	0.614
13.32	19.40	37.2	0.075	0.81	0.512
15.20	21.64	35.0	0.001	0.02	0.01

[a] $\alpha = 0.971$.
[b] Calculated using Chow equation.
[c] C'_H/α = Langmuir site capacity.
[d] C_H/α = concentration of CO_2 in Langmuir mode.

TABLE III
CO_2 Sorption Parameters for PVF_2/PMMA Blends at 35°C

Wt % PVF_2	Volume fraction of PVF_2 in amorphous phase, ϕ_1	Volume fraction of amorphous phase, α	From isotherm slope		From regression analysis		
			k_D [cm³ (STP)/cm³ atm]	k_D/α [cm³ (STP)/cm³ atm]	k_D/α [cm³ (STP)/cm³ atm]	C'_{H0}/α [cm³ (STP)/cm³]	b (atm^{-1})
100	1.0	0.426	0.664	1.559	—	—	—
80	0.556	0.621	0.865	1.394	—	—	—
60	0.387	0.812	1.105	1.362	1.494	7.26	0.0859
50	0.330	0.886	1.215	1.371	—	—	—
40	0.283	0.953	1.283	1.346	1.403	8.15	0.101
35	0.258	0.971	1.319	1.358	1.417	10.9	0.126
20	0.150	1.0	—	—	1.352	16.3	0.103
0	0	1.0	—	—	1.409	25.6	0.0993

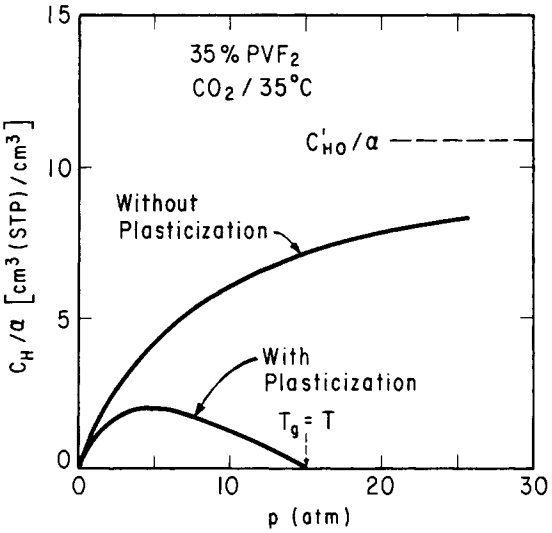

Fig. 6. Concentration of CO_2 in Langmuir mode (per unit volume of amorphous phase) for 35% PVF_2 blend assuming no plasticization occurs and allowing for this via eq. (3).

ory to the present case gives

$$\ln\left(\frac{k_D}{\alpha}\right) = \phi_1 \ln\left(\frac{k_D}{\alpha}\right)_1 + \phi_2 \ln\left(\frac{k_D}{\alpha}\right)_2 + \left(\frac{BV_3}{RT}\right)\phi_1\phi_2 \tag{8}$$

where B is the binary interaction energy density, V_3 is the molar volume of the diluent which is taken as 55 cm^3/mol for CO_2,[56] and ϕ_i is the volume fraction of polymer 1 or 2 in the miscible amorphous phase. The latter are different from the overall blend composition owing to the depletion of the amorphous phase of PVF_2 caused by formation of a separate crystalline phase of this species, and values for ϕ_1 (1 = PVF_2) calculated using the DSC measured levels of crystallinity are listed in Table III. Figure 7 shows the values for the Henry's law coefficient per unit volume of amorphous phase plotted as suggested by eq. (8). The solid line is the best regression fit of the data to eq. (8) and this yields a value of $B = -3.50$ cal/cm^3, which is in good agreement with values estimated for the interaction of PVF_2 with PMMA derived from melting point depression analysis, viz., -2.98[2] and -3.85 cal/cm^3.[9] The values of the Henry's law parameter from the regression of the sorption isotherm are more scattered than those obtained from the isotherm where possible which is not surprising.

The Langmuir capacity term based on unit volume of amorphous phase, C'_{H0}/α, form a linear correlation with ($T_{g0} - T$) (see Fig. 8) as expected based on similar correlations found previously. The affinity parameter b varies little with blend composition as seen in Figure 9. The correlations shown in Figures 7–9 allow simple physical interpretations of the parameters from the modified sorption model.

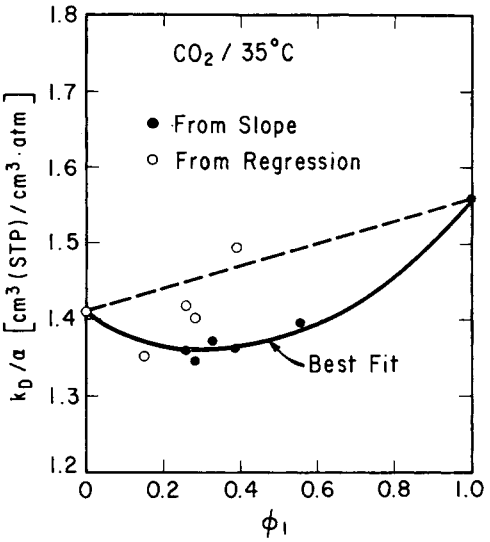

Fig. 7. Correlation of Henry's law coefficient based on volume of amorphous phase, k_D/α, with blend composition expressed as the volume fraction of PVF_2 in the amorphous phase, ϕ_1: (—) best fit to eq. (8); ●) from slope; (○) from regression.

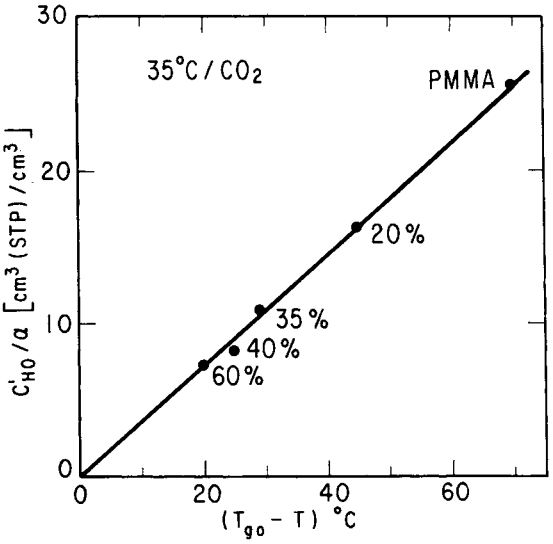

Fig. 8. Correlation of corrected Langmuir site capacity based on volume of amorphous phase, C'_{H0}/α, with $(T_{g0} - T)$ for CO_2 sorption in PVF_2/PMMA blends.

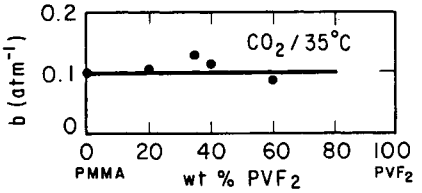

Fig. 9. Dependence of affinity constant b on overall blend composition for CO_2 sorption in PVF_2/PMMA blends.

Permeation

Permeability coefficients for CO_2 in these blends are shown in Figure 10. In every case, the permeability increases with pressure. For rubbery polymers, it is usual to find that the permeability of low solubility gases like He, Ar, N_2, and CH_4 have little if any pressure dependence,[38,57,58] whereas significant increases with pressure are observed commonly[57-60] for higher solubility gases like CO_2. On the other hand, most glassy polymers show a slight *decrease* in permeability with pressure for a range of gases including CO_2.[33,34,40,46,61-66] This behavior is usually interpreted in terms of an extension of the dual sorption approach by a model which envisions separate mobilities for the gas molecules sorbed by the two modes, i.e.,

$$P = k_D D [1 + FK/(1 + bp_2)] \tag{9}$$

where D is the diffusion coefficient for the Henry's law mode, $K = C'_H b / k_D$, and F is the ratio of the diffusion coefficient for the Langmuir mode to D. Both transport coefficients are assumed to be independent of concentration in this formulation, and data for many systems are consistent with this assumption. Most cases result in a small positive value for F, but the special case of total immobilization of the Langmuir population, i.e., $F = 0$, has been considered.[67,68] The transport of Ar, N_2, and CH_4 in PMMA and poly(ethyl methacrylate) (PEMA) to be reported later is well described by eq. (9) with $F = 0$.

It is quite rare to find the permeability of CO_2 to increase with pressure in a glassy polymer. This, however, has been reported previously for PMMA.[69] Similar behavior has been found for water vapor in poly-

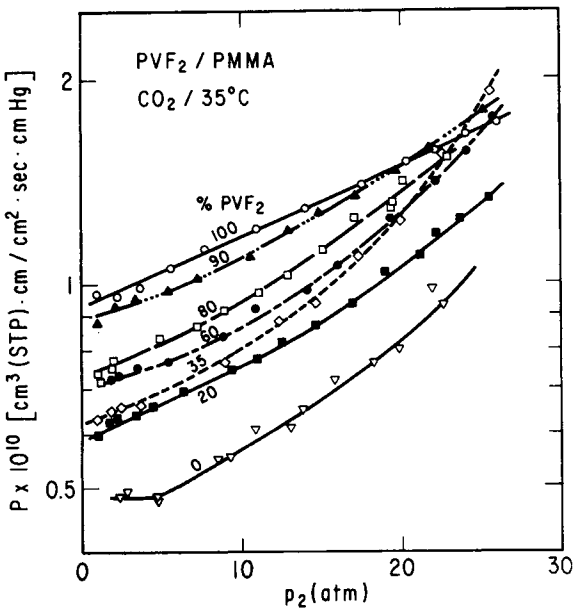

Fig. 10. Pressure dependence of permeability coefficient for CO_2 transport in PVF_2/PMMA blends at 35°C.

acrylonitrile[70-73] and for acetone vapor in ethyl cellulose,[74] which is less surprising owing to the well-recognized potential of these penetrants to plasticize the polymer. In an effort to explore this somewhat unusual result for CO_2, we have recently found similar behavior for CO_2 in PEMA, poly(isobutyl methacrylate), cellulose acetate, and nylon 6. These results and their interpretation will be published later. Here, we will concentrate on simply modelling this behavior for the glassy PMMA–PVF_2 blends.

A formal way of accommodating the present observations to the model embodied in eq. (9) is to consider the transport parameters to be concentration-dependent as a result of plasticization by CO_2. Stern and Saxena[75] have derived a generalized model for permeation in rubbery and glassy polymers by assuming an exponential concentration dependence on the diffusion coefficient

$$D(C_m) = D_0 e^{\xi C_m} \tag{10}$$

where C_m is the concentration of the so-called mobile gas defined earlier as a mathematical convenience for glassy polymers[66] and it includes all of the Henry's law population and the fraction F of the Langmuir population. The parameters D_0 and ξ have obvious meaning. The replacement for eq. (9) becomes[75]

$$P = \frac{D_0}{\xi p_2}\left\{\exp\left[\xi k_D p_2\left(1 + \frac{FK}{1 + bp_2}\right)\right] - 1\right\} \tag{11}$$

For rubbery polymers where $K = 0$ or for glassy polymers with $F = 0$, eq. (11) reduces to

$$P = \frac{D_0}{\xi p_2}\left[\exp(\xi k_D p_2) - 1\right] \tag{12}$$

In principle, the three transport parameters D_0, ξ, and F could be obtained by regression analysis of experimental data. However, for the glassy blends considered here we have set $F = 0$ for two reasons. First, as mentioned earlier transport of Ar, N_2, and CH_4 in the same blends are consistent with a value of $F = 0$. For other glassy polymers,[33,62,76,77] the value of F for CO_2 tends to be even smaller than observed for these gases. Second, we feel that regression for three parameters pushes the data and the model beyond the limits of any statistical meaning. This is illustrated for one data set in Table IV, where F has been arbitrarily set at values between 0 and 1 and D_0 and ξ were obtained by subsequent regression analysis which selects parameters to minimize the objective function

$$Q = \sum_1^N (P_{\text{cald}} - P_{\text{expt}})_i^2 \tag{13}$$

where N is the number of data points, P_{expt} is the experimental permeability, and P_{cald} is the permeability computed from the model, eq. (11) in this case.

TABLE IV
Comparison of CO_2 Transport Parameters D_0 and ξ and variance σ for 20% PVF_2 Blend[a]

F	$D_0 \times 10^9$/ (cm^2/s)	$\xi \times 10^2$ (cm^3/cm^3 (STP))	σ (Barrer)	σ/P_{min} (%)	σ/P_{max} (%)
0	3.17	4.37	0.0248	4.17	1.85
0.134	2.78	4.58	0.0201	3.38	1.50
0.453	2.13	4.83	0.0152	2.55	1.13
0.792	1.68	4.88	0.0142	2.39	1.06
1.0	1.48	4.85	0.0145	2.44	1.08

[a] Data were fitted to eq. (12) with an arbitrarily assigned F value. P_{min} and P_{max} are the minimum and maximum permeability coefficients in the data set.

The variance defined as

$$\sigma = \sqrt{\frac{Q}{N-1}} \tag{14}$$

and its values relative to the minimum and maximum permeabilities in the data set are listed in Table IV for each choice of F. For each assigned F, an optimal set of D_0 and ξ could be found as shown which allows the model to fit the data within the limits of experimental error, about 3%. While a finite value of F gives a little better fit, this may be just the result of another degree of freedom in curve fitting and so we have set $F = 0$ in every case in accord with the physical argument mentioned first. A distinct modelling advantage of this reasonable assumption is that no information is needed about the sorption isotherm beyond the Henry's law part, which is especially important here owing to the complex changes in the Langmuir part of the sorption described above.

Based on the arguments presented above, eq. (12) was adopted as the model for analysis of the permeability data shown in Figure 10. The parameters D_0 and ξ were obtained for each blend by regression analysis, and the values obtained are listed in Table V along with statistical measures of the quality of the fit. Further comments on the latter will be made in subsequent discussions. Figure 11 shows how the D_0 obtained varies with

TABLE V
Transport Parameters from regression analysis for CO_2 in PVF_2/PMMA Blends at 35°C
Assuming $F = 0$ for Glassy Blends

Wt % PVF_2	$D_0 \times 10^9$ (cm^2/s)	$\xi \times 10^2$ [cm^3/cm^3 (STP)]	$(D_0/\alpha) \times 10^9$ (cm^2/sec)	$\alpha\xi \times 10^2$ [cm^3/cm^3 (STP)]	σ[a] (Barrer)	σP_{10}(%)[b]
100	10.65	6.65	25.0	2.84	0.016	1.4
90	8.53	7.07	16.5	3.65	0.019	1.7
80	6.11	7.06	9.83	4.38	0.025	2.7
60	4.40	5.91	5.42	4.80	0.055	6.4
35	3.05	6.22	3.14	6.04	0.075	9.4
20	3.17	4.37	3.17	4.37	0.025	3.3
0	2.22	4.53	2.22	4.53	0.031	5.5

[a] σ = variance defined by eqs. (13) and (14).
[b] Variance relative to permeability at 10 atm expressed as a percentage.

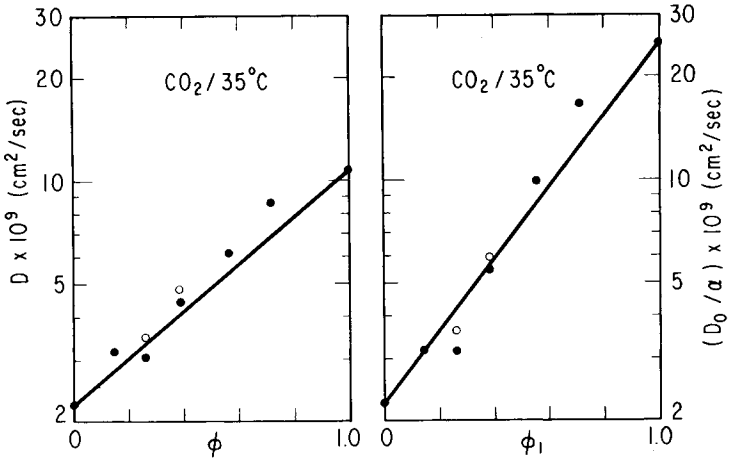

Fig. 11. Diffusion coefficients for CO_2 at $C = 0$, obtained by fitting data to model, as a function of volume fraction of PVF_2 in amorphous phase. Plot on right makes approximate correction for crystallinity (assumes $\kappa = \alpha$): (●) based on data over full pressure range (Table V); (○) obtained from limited pressure range (Table VI).

volume fraction of PVF_2 in the amorphous phase; however, the representation on the left makes no allowance for the influence of the variable level of crystallinity in these blends (see Fig. 2). Because of the impermeability of the crystalline phase, the diffusion coefficients given by eq. (10) are apparent ones which are related by a structure factor[52,77] κ to the actual diffusion coefficient of the amorphous phase D_a where all transport occurs:

$$D = \kappa D_a \tag{15}$$

The structural factor is less than unity and depends on the volume fraction of crystals, their shape, and their organization in the amorphous phase. Earlier studies[78] have suggested that κ can be approximated as the volume fraction of the amorphous phase, i.e.,

$$\kappa \simeq \alpha \tag{16}$$

This is no doubt an oversimplification, and in most cases κ is probably less than this. However, in the absence of any relationship, we will adopt this approximation. As a further point, the concentration in the exponent of eq. (10) should be based on the volume of the amorphous phase when the material is crystalline. Combining each of these issues results in

$$D_a = \frac{D_0}{\alpha} \exp\left[\alpha\xi\left(\frac{C_m}{\alpha}\right)\right] \tag{17}$$

Thus, D_0/α and $\alpha\xi$ listed in Table V are the more appropriate parameters for semicrystalline materials. The right-hand side of Figure 11 shows D_0/α vs. the volume fraction of PVF_2 in the amorphous phase. The trend is somewhat improved by this adjustment; however, owing to the limitations

of the inherently approximate nature of eq. (16) and the as-yet unknown effect of film orientation,[79] a detailed interpretation or comparison with similar relations for amorphous blends[34-39] is not warranted.

Using eq. (16) and the fact that CO_2 is not soluble in the crystalline phase [see eq. (7)], the permeability in the amorphous phase of these blends is estimated to be

$$P_a = P/\alpha^2 \tag{18}$$

The results calculated from the data in Figure 10 and Table III are plotted in Figure 12. Here we have reversed the use of logarithmic and arithmetic coordinates from that employed in Figure 10 to emphasize the difference in the method of presentation. Figure 12 exaggerates the leveling off of permeability coefficients at low pressures. Stern and Saxena[75] demonstrated that a model like eq. (11) might show a slight minimum on such coordinates if F were not zero.

Equations (11) or (12) may be rewritten in terms of an integral diffusion coefficient as follows:

$$P = k_D\bar{D}[1 + FK/(1 + bp_2)] \tag{19}$$

where the integral diffusion coefficient is defined by

$$\bar{D} = \frac{1}{C_{m2}}\int_0^{C_{m2}} D(C_m)\, dC_m \tag{20}$$

where C_{m2} is the mobile concentration at the upstream membrane surface

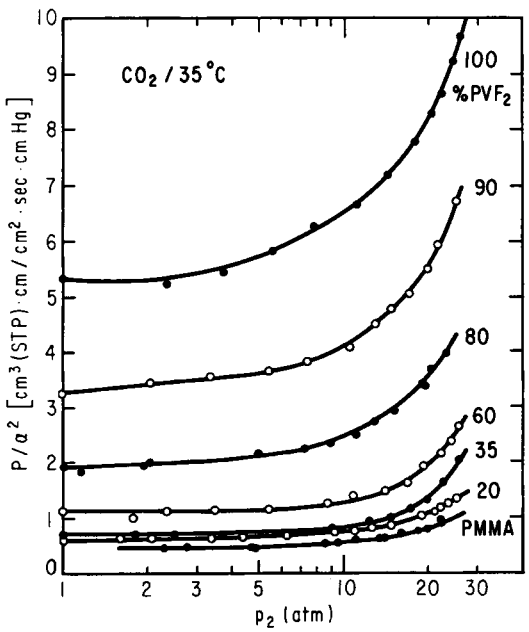

Fig. 12. Estimated amorphous phase permeability coefficients as a function of pressure.

which is in equilibrium with p_2. In the case of eq. (10), we obtain

$$\overline{D} = \frac{D_0}{\xi C_{m2}} [\exp(\xi C_{m2}) - 1] \tag{21}$$

Figure 13 shows $\overline{D}$ calculated from the experimental permeability data using eq. (19) with the assumption that $F = 0$ (thus only information about k_D is needed). The lines show the results computed from the model using the parameters listed in Table V. For simplicity, these are apparent values not adjusted for crystallinity which in no way affects the comparison as may be seen above. The fit is quite good except for the extreme case of the 35% PVF_2 blend. The values of the variance listed in Table V show this in another way.

The relatively poorer fit of the model to the data for the 35% PVF_2 blend (see large variance in Table V) stems from the unusually steep pressure dependence the permeability exhibits at high pressure. Beyond 15 atm, the upstream layers of this film will have its T_g depressed below 35°C by CO_2 plasticization while the lower concentrations of CO_2 further downstream in the film will leave this material in the glassy state. Owing to the effect of traversing the T_g on transport behavior,[43,80-82] one cannot expect simple models like the present one to accommodate such a complex situation. Table VI shows the results for a fit of the model to permeability data below 15 atm. The resulting variance is reduced to the level of those shown for other blends in Table V, and more reasonable transport parameters are obtained.

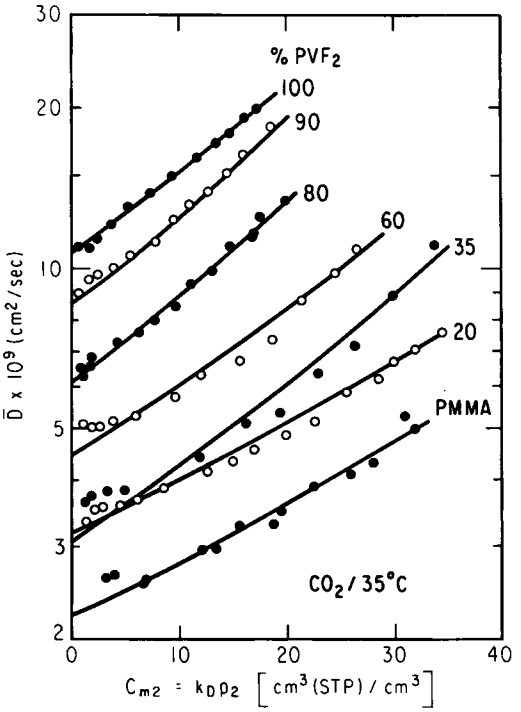

Fig. 13. Integral diffusion coefficients versus upstream concentration of mobile CO_2 (assumes $F = 0$). Points are experimental data while solid lines are best fits from model.

TABLE VI
Results of Regression Analyses Using Data over Pressure Ranges Shown for Two Blends Which Change from Glassy to Rubbery States in Permeation Measurement

Wt % PVF_2	Pressure range used in regression (atm)	$D_0 \times 10^9$ (cm^2/s)	$\xi \times 10^2$ [cm^3/cm^3 (STP)]	$(D_0/\alpha) \times 10^9$ (cm^2/s)	$\alpha\xi \times 10^2$ [cm^3/cm^3 (STP)]	σ (Barrer)	σ/P_{10}
60	1-26	4.40	5.91	5.42	4.80	0.055	6.4%
	1-15	4.79	4.03	5.90	3.27	0.018	2.0
35	1-26	3.05	6.22	3.14	6.04	0.075	9.4
	1-15	3.50	4.11	3.60	3.99	0.012	1.5

To a lesser extent, similar problems occur for the 60% PVF_2 blends, and again better fitting is obtained when the pressure range used is limited to 15 atm.

Sorption Kinetics

Generally, our sorption apparatus[40,41] is only used to obtain the equilibrium sorption isotherm. However, as shown here, it can also be used to obtain information on the kinetics of sorption. The experiments were carried out from low to high pressures sequentially by introducing a higher pressure at $t = 0$ into the sorption chamber where the polymer had been previously equilibrated with a lower pressure. The pressure decays with time to a new final equilibrium value since the chamber has a limited volume, and the fractional increase in mass uptake, M_t/M_∞, can be computed as a function of time from the pressure record. The results obtained for a 35% PVF_2 blend film are shown in Figure 14. The legend shows the initial ($t < 0$) and final ($t = \infty$) equilibrium concentrations of CO_2 in the sample along with the concentration at the film surface immediately after raising the pressure ($t = 0$). The latter corresponds to a point on the sorption isotherm at the new pressure before any decay occurs. This situation represents a complex boundary condition; however, the following equation,[83]

$$\frac{M_t}{M_\infty} = \frac{4}{l}\sqrt{\frac{Dt}{\pi}} \tag{22}$$

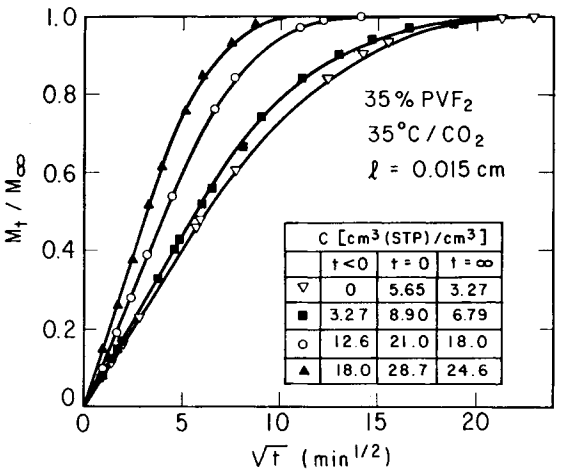

Fig. 14. Sorption kinetics for CO_2 in 35% PVF_2 blend. Legend shows equilibrium concentrations at $t < 0$ and $t = \infty$ and the surface concentration at $t = 0$ for each experiment.

	C [cm³ (STP)/cm³]		
	$t < 0$	$t = 0$	$t = \infty$
▽	0	5.65	3.27
■	3.27	8.90	6.79
○	12.6	21.0	18.0
▲	18.0	28.7	24.6

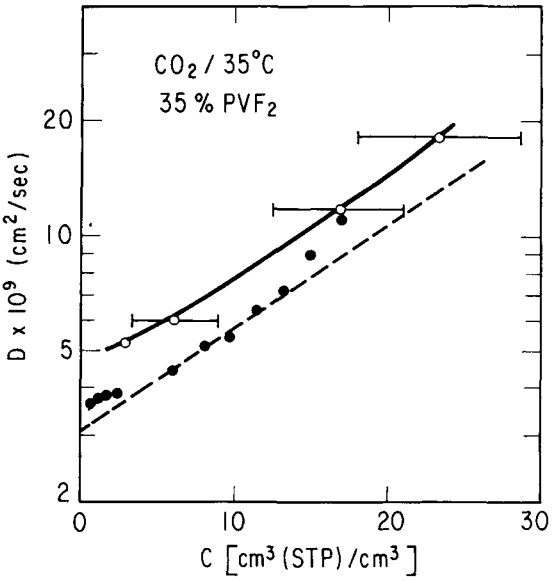

Fig. 15. Diffusion coefficients for CO_2 in 35% PVF_2 blend: (○) computed from sorption kinetics—bars show range of C from legend in Figure 14; (●) integral diffusion coefficients from Figure 13 plotted at $C = C_{m2}/2$; (- - -) differential diffusion coefficients computed from eq. (10) and parameters in Table V.

where l is the film thickness, can be used to compute an approximate differential diffusion coefficient from the initial slopes in Figure 14. The results are plotted vs. the average concentration in Figure 15, and agreement with differential diffusion coefficients computed from permeation data [eq. (10)] is quite good in view of the difficulties mentioned earlier for this particular blend.

SUMMARY

It has been demonstrated here that high pressure CO_2 sorption and permeation in PVF_2/PMMA blends involve several complex phenomena. However, the behavior has been modelled rather successfully using appropriate extension of previously developed models. The glass transition temperature curve for these blends crosses the observation temperature of 35°C so that blends rich in PMMA are glassy while those rich in PVF_2 are rubbery. Blends rich in PVF_2 are also semicrystalline while those rich in PMMA are amorphous. Carbon dioxide plasticizes these blends and reduces their T_g's. Some intermediate compositions were glassy at low CO_2 pressures but became rubbery, because of CO_2 plasticization, at higher pressures. In these cases the CO_2 sorption isotherm is curved at low pressures as expected for glassy polymers but becomes linear at higher pressures where the T_g has become less than the observation temperature. Plasticization by CO_2 can induce further PVF_2 crystallization. PMMA is unusual for a glassy polymer in that its permeability to CO_2 *increases* with pressure owing to plasticization.

The dual sorption model was modified to allow for the influence of changes in the Langmuir capacity term as T_g decreases on CO_2 sorption and was successfully applied to blends which were glassy. This modified model gives

a satisfactory description for systems where CO_2 sorption converts the originally glassy material into a rubbery one. Transport behavior was modelled using a concentration dependent diffusion coefficient in the dual mobility model as suggested by Stern and Saxena.[75] Other models for sorption and transport[84,85] are available, but they lack simple physical interpretations. The effects of crystallinity variations with blend composition on both sorption and transport behavior were accounted for in the model.

A large number of glassy polymers show a decrease in CO_2 permeability with pressure; thus the trends seen here for PMMA are regarded as unusual. The reasons for this are of great interest and further investigations on this point are in progress.

This research was sponsored by the U. S. Army Research Office.

References

1. J. S. Noland, N. N. C. Hsu, R. Saxon, and J. M. Schmitt, *Adv. Chem. Ser.*, **99**, 15 (1971).
2. T. Nishi and T. T. Wang, *Macromolecules*, **8**, 909 (1975).
3. D. R. Paul and J. O. Altamirano, *Adv. Chem. Ser.*, **142**, 371 (1975).
4. T. K. Kwei, H. L. Frisch, W. Radigan, and S. Vogel, *Macromolecules*, **10**, 157 (1977).
5. R. E. Bernstein, C. A. Cruz, D. R. Paul, and J. W. Barlow, *Macromolecules*, **10**, 681 (1977).
6. G. DiPaola-Baranyi, S. J. Fletcher, and P. Degre, *Macromolecules*, **15**, 885 (1982).
7. T. T. Wang and T. Nishi, *Macromolecules*, **10**, 421 (1977).
8. F. A. Bovey, F. C. Schilling, T. K. Kwei, and H. L. Frisch, *Macromolecules*, **10**, 559 (1977).
9. D. R. Paul, J. W. Barlow, R. E. Bernstein, and D. C. Wahrmund, *Polym. Eng. Sci.*, **18**, 1225 (1978).
10. B. S. Morra and R. S. Stein, *J. Polym. Sci., Polym. Phys. Ed.*, **20**, 2243 (1982).
11. B. S. Morra and R. S. Stein, *J. Polym. Sci., Polym. Phys. Ed.*, **20**, 2261 (1982).
12. J. Mijoric, H. L. Luo, and C. D. Han, *Polym. Eng. Sci.*, **22**, 234 (1982).
13. S. R. Murff, J. W. Barlow, and D. R. Paul, *Adv. Chem. Ser.*, **211**, 313 (1986).
14. J. S. Chiou, J. W. Barlow, and D. R. Paul, *J. Appl. Polym. Sci.*, **30**, 2633 (1985).
15. J. S. Chiou, J. W. Barlow, and D. R. Paul, *J. Appl. Polym. Sci.*, **30**, 3911 (1985).
16. R. P. Kambour, C. L. Gruner, and E. E. Romagosa, *Macromolecules*, **7**, 248 (1974).
17. R. P. Kambour and C. L. Gruner, *J. Polym. Sci., Polym. Phys. Ed.*, **16**, 703 (1978).
18. A. B. Desai and G. L. Wilkes, *J. Polym. Sci., Polymer Symp.*, **46**, 291 (1974).
19. H. Jameel, J. Waldman, and L. Rebenfeld, *J. Appl. Polym. Sci.*, **26**, 1795 (1981).
20. S. B. Lin and J. L. Koenig, *J. Polym. Sci., Polym. Phys. Ed.*, **21**, 1539 (1983).
21. E. Turka and W. Benechi, *J. Appl. Polym. Sci.*, **23**, 3489 (1979).
22. R. A. Ware, S. Tirtowidjojo, and C. Cohen, *J. Appl. Polym. Sci.*, **26**, 2975 (1981).
23. J. S. Chiou, Y. Maeda, and D. R. Paul, *J. Appl. Polym. Sci.*, **30**, 4019 (1985).
24. R. A. Assink, *J. Polym. Sci., Polym. Phys. Ed.*, **12**, 2281 (1974).
25. W. V. Wang, E. J. Kramer, and W. H. Sachse, *J. Polym. Sci., Polym. Phys. Ed.*, **20**, 1371 (1982).
26. B. G. Ranby, *J. Polym. Sci. Symp.*, **51**, 89 (1975).
27. Y. J. Shur and B. Ranby, *J. Appl. Polym. Sci.*, **19**, 1337 (1975).
28. Y. J. Shur and B. Ranby, *J. Appl. Polym. Sci.*, **19**, 2143 (1975).
29. Y. J. Shur and B. Ranby, *J. Appl. Polym. Sci.*, **20**, 3105 (1976).
30. Y. J. Shur and B. Ranby, *J. Appl. Polym. Sci.*, **20**, 3121 (1976).
31. Y. J. Shur and B. Ranby, *J. Macromol. Phys.*, **B14**, 565 (1977).
32. H. B. Hopfenberg and D. R. Paul, in *Polymer Blends*, D. R. Paul and S. Newman, Eds. Academic, New York, 1978, Vol. I, Chap. 10.
33. P. Masi, D. R. Paul, and J. W. Barlow, *J. Polym. Sci., Polym. Phys. Ed.*, **20**, 15 (1982).
34. G. Morel and D. R. Paul, *J. Membr. Sci.*, **10**, 273 (1982).
35. J. E. Harris, D. R. Paul, and J. W. Barlow, *Polym. Eng. Sci.*, **23**, 676 (1983).
36. H. G. Spencer and J. A. Yavorsky, *J. Appl. Polym. Sci.*, **28**, 2937 (1983).
37. D. R. Paul, *J. Membr. Sci.*, **18**, 75 (1984).
38. J. S. Chiou and D. R. Paul, *J. Appl. Polym. Sci.*, **30**, 1173 (1985).

39. Y. Maeda and D. R. Paul, *Polymer*, **26**, 2055 (1985).
40. W. J. Koros, D. R. Paul, and A. A. Rocha, *J. Polym. Sci., Polym. Phys. Ed.*, **14**, 687 (1976).
41. W. J. Koros and D. R. Paul, *J. Polym. Sci., Polym. Phys. Ed.*, **14**, 1903 (1976).
42. R. F. Boyer, *J. Polym. Sci., Polym. Symp. Ed.*, **50**, 189 (1975).
43. M. Fujii, V. Stannett, and H. B. Hopfenberg, *J. Macromol. Sci.-Phys.*, **B15**, 421 (1978).
44. G. J. Welch and R. L. Miller, *J. Polym. Sci., Polym. Phys. Ed.*, **14**, 1683 (1976).
45. W. R. Vieth, J. M. Howell, and J. H. Hsieh, *J. Membr. Sci.*, **1**, 177 (1976).
46. D. R. Paul, *Ber. Bunsenges. Phys. Chem.*, **83**, 294 (1979).
47. W. J. Koros and D. R. Paul, *J. Polym. Sci., Polym. Phys. Ed.*, **16**, 1947 (1978).
48. A. G. Wonders and D. R. Paul, *J. Membr. Sci.*, **5**, 63 (1979).
49. A. H. Chan and D. R. Paul, *Polym. Eng. Sci.*, **20**, 87 (1980).
50. Y. Maeda, Ph.D. dissertation, University of Texas at Austin, 1985.
51. K. Toi, G. Morel, and D. R. Paul, *J. Appl. Polym. Sci.*, **27**, 2997 (1982).
52. K. Toi and D. R. Paul, *Macromolecules*, **15**, 1104 (1982).
53. T. S. Chow, *Macromolecules*, **13**, 362 (1982).
54. A. S. Michaels and H. J. Bixler, *J. Polym. Sci.*, **50**, 393 (1961).
55. A. S. Michaels and R. B. Parker, Jr., *J. Polym. Sci.*, **41**, 53 (1959).
56. J. M. Prausnitz and F. H. Shair, *AIChE J.*, **6**, 682 (1961).
57. S. A. Stern, S. M. Fang and R. M. Jobbins, *J. Macromol. Sci.-Phys.*, **B5**, 41 (1971).
58. S. A. Stern and S. M. Fang, *J. Polym. Sci., A-2*, **10**, 201 (1972).
59. N. N. Li and E. J. Henley, *AIChE J.*, **10**, 666 (1964).
60. R. A. Assink, *J. Polym. Sci., Polym. Phys. Ed.*, **15**, 227 (1977).
61. W. J. Koros, D. R. Paul, M. Fujii, H. B. Hopfenberg, and V. Stannett, *J. Appl. Polym. Sci.*, **21**, 2899 (1977).
62. W. J. Koros, A. H. Chan, and D. R. Paul, *J. Membr. Sci.*, **2**, 165 (1977).
63. A. H. Chan, W. J. Koros, and D. R. Paul, *J. Membr. Sci.*, **3**, 117 (1978).
64. G. S. Hurvard, V. T. Stannett, W. J. Koros, and H. B. Hopfenberg, *J. Membr. Sci.*, **6**, 185 (1980).
65. J. H. Petropoulos, *J. Polym. Phys., A-2*, **8**, 1797 (1970).
66. W. J. Koros and D. R. Paul, *J. Polym. Sci., Polym. Phys. Ed.*, **14**, 675 (1976).
67. D. R. Paul, *J. Polym. Sci., A-2*, **7**, 1811 (1969).
68. D. R. Kemp and D. R. Paul, *J. Polym. Sci.*, **41C**, 79 (1973).
69. G. B. Okonishinikov and V. P. Skripov, *Vysokmol. Soedin., Ser. B*, **15**, 890 (1973).
70. G. R. Mauze and S. A. Stern, *J. Membr. Sci.*, **12**, 51 (1982).
71. G. R. Mauze and S. A. Stern, *Polym. Eng. Sci.*, **10**, 548 (1983).
72. V. T. Stannett, M. Haider, W. J. Koros, and H. B. Hopfenberg, *Polym. Eng. Sci.*, **20**, 300 (1980).
73. V. T. Stannett, G. R. Ranade, and W. J. Koros, *J. Membr. Sci.*, **10**, 219 (1982).
74. V. Saxena and S. A. Stern, *J. Membr. Sci.*, **12**, 65 (1982).
75. S. A. Stern and V. Saxena, *J. Membr. Sci.*, **7**, 47 (1980).
76. A. J. Erb and D. R. Paul, *J. Membr. Sci.*, **8**, 11 (1981).
77. A. S. Michaels and H. J. Bixler, *J. Polym. Sci.*, **50**, 413 (1961).
78. R. M. Barrer, in *Diffusion in Polymers*, J. Crank and G. S. Park, Eds., Academic, New York, 1968, Chap. 6.
79. M. J. El-Hibri, Ph.D. dissertation, Univeristy of Texas at Austin, 1985.
80. W. H. Burgess, H. B. Hopfenberg, and V. T. Stannett, *J. Macromol. Sci.-Phys.*, **B5**, 23 (1971).
81. S. A. Stern, S. K. Sen, and A. K. Rao, *J. Macromol. Sci.-Phys.*, **B10**, 507 (1974).
82. K. Toi, Y. Maeda, and T. Tokuda, *J. Membr. Sci.*, **13**, 15 (1983).
83. J. Crank and G. S. Park, in *Diffusion in Polymers*, J. Crank and G. S. Park, Eds., Academic, New York, 1968, Chap. 1.
84. D. Raucher and M. D. Sefcik, *Am. Chem. Soc. Symp. Ser.*, **223**, 89 (1983).
85. D. Raucher and M. D. Sefcik, *Am. Chem. Soc. Symp. Ser.*, **223**, 111 (1983).

Received April 3, 1985
Accepted December 17, 1985